Pol. J. Food Nutr. Sci., 2021, Vol. 71, No. 1, pp. 39–50
On-line ISSN: 2083-6007
Print ISSN: 1230-0322
DOI: 10.31883/pjfns/132064
http://journal.pan.olsztyn.pl

Original article
Section: Food Quality and Functionality

Enhancement of the Stabilities and Intracellular Antioxidant Activities of Lavender Essential Oil by Metal-Organic Frameworks Based on β-Cyclodextrin and Potassium Cation

Ying Wang, Liang Wang, Jin Tan, Rong Li, Zi-Tao Jiang, Shu-Hua Tang*

Tianjin Key Laboratory of Food Biotechnology, College of Biotechnology and Food Science, Tianjin University of Commerce, Tianjin 300134, China

Key words: microcapsulation, thermal stability, pH stability, cell viability, cellular antioxidant model, application extension

Lavender (*Lavandula angustifolia*) is an important medicinal and aromatic plant. However, the application of lavender essential oil (LEO) is limited by its instability, low solubility and high volatility. Therefore, to improve the stabilities and antioxidant activities of LEO and thereby expand the applications, LEO was microencapsulated by metal-organic frameworks based on β-cyclodextrin and potassium cation (K-βCD-MOFs) with different mass core/wall ratios. The results showed that the best inclusion rate was 96.67% with the ratio of 1:10. Then, the optimum inclusion product was characterized by Fourier transform infrared spectroscopy (FTIR) and scanning electron microscope (SEM). The thermal and pH stabilities and the intracellular antioxidant activities were also studied. The results showed that the stabilities of the oil with K-βCD-MOFs inclusions and their abilities to resist acid and alkali were significantly stronger than those of LEO itself. In addition, the intracellular antioxidant activities of LEO were also enhanced by the K-βCD-MOFs inclusion. These results suggested the potential of K-βCD-MOFs as carriers for essential oils in food industry applications.

INTRODUCTION

Lavender (*Lavandula angustifolia*), an aromatic plant belonging to the family Lamiaceae, is widely grown for essential oil production due to its aromatic property [Shafaei *et al.*, 2017]. This herbal plant is commonly utilized in many industrial fields including cosmetics, perfumes, pharmaceuticals, and foods [Yuan *et al*., 2019]. Taking foods as an example, it is widely used as flavoring in beverages, herbal teas, ice creams, sweets, cakes, and other aromatic plant products [Dong *et al*., 2020]. Essential oil, the most important and popular product of this aromatic plant, mainly exists in the glands of the aerial parts including flowers and leaves [Lis-Balchin, 2002]. The lavender essential oil (LEO) is believed to have anti-depressive, anti-inflammatory, antimicrobial (antibacterial/ antifungal) and antioxidant characteristics [Cavanagh & Wilkinson, 2005; Insawang *et al*., 2019; Kwiatkowski *et al*., 2020]. LEO is also prevalent in the pharmaceutical, cosmetic and food industries. However, the applications of LEO are limited by its highly unstable and volatile properties. As the essential oils are composed of various volatile and lipophilic components, they are susceptible to light, heat and air, and thus to conversion and degradation [Yuan *et al*., 2019]. Beyond that, their poor stabilities also lead to difficult storage and transportation.

Consequently, stability enhancement methods of LEO are essential to expand the applications. Microencapsulation technologies for essential oil have raised concern in biology, medicine and food researches in the last few years. As common wall materials for microencapsulation, cyclodextrins (CDs) are a class of cyclic oligosaccharides normally produced from starch under the effect of the enzyme catalytic reaction [Thombre *et al*., 2013]. CDs are characterized by their amphiphilic structure with hydrophobic inner cavity and hydrophilic outer wall, which could embed guest molecules to form relatively stable complexes [Tian *et al*., 2020]. They are mainly composed of 6, 7 or 8 glucose units, known as α-, β- and γ-CD, respectively [Thombre *et al*., 2013]. Among them, β-CD is one of the most important members and is derived from 7 D(+)-glucose units linked by α-1,4-glycosidic bonds [Thombre *et al*., 2013]. Comparing with other CDs, β-CD is the most frequently used CD due to the lowest price and relatively appropriate size cavity. The interest in β-CD regarding its food-related applications has been increasing since it was approved for food uses by FDA [Partanen *et al*., 2002]. With cavity, β-CD could act as a host and include some molecules as guests to form inclusion complexes by van der Waals and hydrophobic interaction forces, or hydrogen bonds [Deng *et al*., 2018]. However, the applications of β-CD are limited by its relatively low binding capacity and solubility. Therefore, the metal-organic frameworks (MOFs) with the utilization of the special structure of CDs were developed to solve the above problems. CD-MOFs are network-structure and crystalline porous materials derived from CDs and metal ions or clusters for biomedical applications [Li *et al*., 2017; Smaldone *et al*., 2010]. They have high porosity, large surface areas, and ver-

* Corresponding Author e-mail: tanjin@tjcu.edu.cn (J. Tan).

satility in terms of composition and functionalities [Li & Huo, 2015]. Particularly, K-βCD-MOFs could be synthesized from β-CD and K ions employing a vapor diffusion method [Smaldone *et al*., 2010]. The K-βCD-MOFs have good cutting structure, high drug loading capacity and strong inclusion ability, in addition, they are environment-friendly, biocompatible and without side-effects on the human body [Abuçafy *et al*., 2018; Liu *et al*., 2017]. Kumar *et al*. [2020] reviewed that MOFs could be widely applied to various areas including catalysis, energy storage, solar cells, air and water purification, gas storage, bioimaging, drug delivery, waste remediation and sensors. So far, MOFs are rarely applied in food, however, K-βCD-MOFs are recognized due to their non-toxicity and unique "food-grade synthesis" based on natural components [Kumar *et al*., 2020]. Therefore, the potential of K-βCD-MOFs as microcapsule wall materials is huge and the application prospects are also broad, especially possible in food.

To our best knowledge, limited researches were done on the essential oil stability improvement using CDs or MOFs related materials. For example, Yuan *et al*. [2019] reported LEO encapsulated in hydroxypropyl-β-cyclodextrin (HPCD) and Wu *et al*. [2019] investigated zinc metal-organic framework (Zn@MOF) as a carrier for thymol. There is no research hitherto on the stability improvement of LEO by microencapsulation by K-βCD-MOFs. Furthermore, whether the microencapsulation by K-βCD-MOFs affects the antioxidant activities of LEO is also important for further applications of the oil. Therefore, LEO was microencapsulated by K-βCD-MOFs to improve the stability and thereby expand the applications. The thermal/pH stabilities and intracellular antioxidant activities were also determined and compared, and the inclusion compound was further identified by Fourier transform infrared spectroscopy (FTIR) and scanning electron microscopy (SEM).

MATERIALS AND METHODS

Apparatus

A blade homogenizer A10 (IKA, Staufen, Germany) was used to ground the plants. An ultrasonic-microwave assisted extraction (UMAE) apparatus CW-2000 (Xintuo, Shanghai, China) was used for the extraction of lavender essential oil. The absorbances for the inclusion rate and stability measurement were determined by an ultraviolet and visible spectrophotometer Lambda25 (PerkinElmer, Waltham, MA, USA). Cell proliferation was measured using a SpectraMax M5 96-well plate reader (Molecular Devices, Sunnyvale, CA, USA). A Fourier transform infrared spectroscope IRAffinity-1 (Shimadzu, Tokyo, Japan) and a scanning electron microscope JSM-IT300 (JEOL, Tokyo, Japan) were used to characterize the essential oil included in the molecular microcapsules. Morphological characteristics of β-CD and K-βCD-MOFs were observed and photographed by an optical microscope (Smart, Chongqing, China).

Chemicals

β-CD and dimethylsulfoxide (DMSO) were purchased from Tianjin Chemical Factory (Tianjin, China). HeLa cells were purchased from the Institute of Biochemistry and Cell Biology (Shanghai, China). The fetal bovine serum (FBS) and Dulbecco's modified eagle's medium (DMEM) were obtained from Gibco Co. (Carlsbad, CA, USA). Double-antibody (penicillin-streptomycin) was purchased from HyClone Co. (South Logan, UT, USA). Methyl thiazolyl tetrazolium (MTT) was purchased from Solarbio Biotechnology Co. (Beijing, China). 2',7'-Dichlorofluorescein diacetate (DCFH-DA) assay kit was purchased from Beyotime Institute of Biotechnology (Shanghai, China). Distilled water was used throughout the experiment. KBr was of spectral purity and was purchased from Tianjin Chemical Factory (Tianjin, China). Other chemicals or reagents were all of analytical grade.

Plant materials and essential oil extraction

The lavender (*Lavandula angustifolia)* aerial parts were purchased from Xinjiang province, China. The plants were ground, sieved to 40 mesh, and stored in cool and dry place. LEO was then extracted by ultrasonic-microwave assisted extraction (UMAE) following our previous work [Wang *et al*., 2018] with modifications. The extraction temperature, microwave power, ultrasonic power, extraction time and the ratio of plant material to liquid were 100°C, 600 W, 50 W, 7 min and 1:10 (g/mL), respectively. The mean values of the LEO yields were 3.27% based on dry weights.

Synthesis of K-βCD-MOFs

The high purity β-CD crystals were obtained by the following steps. First, β-CD was dissolved in distilled water heated to 85°C to form a saturated solution, cooled down, and then the crystals were collected by filtration. The above operation was repeated three times and the crystals were combined and oven-dried at 100°C.

K-βCD-MOFs were synthesized based on the above purified β-CD crystals according to the methanol vapor diffusion method with some modifications [Smaldone *et al*., 2010]. Briefly, 1.1349 g of purified β-CD were dissolved with 0.4488 g of potassium hydroxide (KOH) in distilled water. This solution was transferred into a beaker after filtration and then sealed in a tank with 100 mL of methanol for one week. This operation aimed to allow the vapor of methanol diffuse into the solution and form K-βCD-MOFs. The formed K-βCD-MOFs are relatively rectangular, colorless and transparent crystals. The K-βCD-MOFs crystals were then washed twice with 30 mL of methanol. K-βCD-MOFs and β-CD were observed under an optical microscope for their basic morphological characteristics.

Formation of LEO/β-CD and LEO/K-βCD-MOFs inclusion complexes

The lavender essential oil (LEO) as a core was microencapsulated by K-βCD-MOFs as wall materials to form the inclusion complexes by different mass core/wall ratios (1:3, 1:5, 1:8, 1:10 and 1:12) following Michida *et al*. [2015] with modification. Briefly, 1 mg/mL of the LEO solution was prepared by dissolving the oil in 45% ethanol, while K-βCD--MOFs were dissolved in isovolumetric distilled water. The oil solution was then added and dispersed into the β-CD-MOFs solution dropwise with stirring at 48°C to ensure thorough mixing and optimum inclusion. The mixture was cooled down

and freeze-dried to obtain the white powdered inclusion complex product. The inclusion rate was calculated as follows:

$$\text{Inclusion rate (\%)} = (1 - \text{As}_{\text{LEO}}/\text{At}_{\text{LEO}}) \times 100\% \quad (1)$$

where: As_{LEO} and At_{LEO} were the amount of LEO on the surface of inclusion complex and the total amount of LEO in the inclusion complex, respectively. The former was calculated by the following steps: 0.05 g of LEO/K-βCD-MOFs powder with each mass core/wall ratio was transferred into a 100 mL volumetric flask, and anhydrous ether was added, then the sample was shaken and made up to the volume. After sufficient mixing, the surface of the complex powder was thoroughly washed. After filtration, the absorbance of the supernatant was measured at 233 nm, which is the maximum absorption wavelength of LEO. At_{LEO} was determined as follows: 0.05 g of LEO/K-βCD-MOFs powder with each mass core/wall ratio was ultrasonically (60 W) dissolved by 100 mL of 45% ethanol for 30 min. After thorough dissolution and filtration, the absorbance of the supernatant was also measured at 233 nm. Both the amounts of the surface and total LEO were calculated using a standard curve of linalool, which is the main component of LEO [Dong *et al*., 2020]. The inclusion rate was also optimized by comparison among different mass core/wall ratios. The LEO/β-CD inclusion complex was also produced according to the previous steps with the core/wall ratio of 1:10, which was the optimum ratio for the LEO/K-βCD-MOFs production.

Properties of LEO, LEO/β-CD and LEO/K-βCD-MOFs

Thermal stability and pH stability measurements

The LEO, LEO/β-CD and LEO/K-βCD-MOFs solutions were prepared by dissolving them in 45% ethanol. Their concentration was 0.1 mg/mL (LEO equivalence). The actual concentrations of the latter two complexes were ten-fold of LEO, as the mass optimum core/wall ratio was 1:10. The three solutions were stored in an oven at 90°C in dark for 10 days. The absorbances of the above solutions were measured at 233 nm every 24 h to study the change of LEO amounts. The preservation rates of LEO, LEO/β-CD and LEO/K-βCD-MOFs to the original LEO amounts were calculated using the following equation:

$$\text{Preservation rate (\%)} = A_{\text{thermal}}/A_c \times 100\% \quad (2)$$

where: A_{thermal} was the absorbance of LEO after heating, while A_c was the absorbance of LEO control sample without temperature treatment.

The pH values of LEO, LEO/β-CD and LEO/K-βCD-MOFs solutions were adjusted by phosphate buffer to 3, 7 and 10, respectively. The three solutions were prepared as mentioned above. The adjusted solutions were stored in the dark at 25°C for 10 days. The absorbances of the solutions were measured at 233 nm every 24 h to study the change of LEO amounts. The preservation rates of LEO, LEO/β-CD and LEO/K-βCD-MOFs to the original LEO amounts were calculated similarly to the above equation mentioned in the thermal stability measurement.

Intracellular antioxidant activity

No mycoplasma contaminations of HeLa cells were guaranteed by using Young *et al*.'s [2010] mycoplasma testing method. The cell viability and intracellular antioxidant activity were measured according to the previous method described in our earlier works [Wang *et al*., 2019; Yang *et al*., 2013] with some modifications. HeLa cells were transferred into a 96-well plate at a density of 1×10^5 per well in 100 μL of growth medium. The growth medium was pre-prepared by mixing 45 mL of DMEM, 5 mL of FBS and 500 μL of double-antibody. Cells were incubated with 5% CO_2 for 24 h at 37°C. After removal of the medium, the cells were washed by a phosphate buffer solution (PBS) (pH=7.4), and then treated with 100 μL of different concentrations (0.001–2 μL/mL, LEO equivalence) of LEO or included LEO (LEO/β-CD and LEO/K-βCD-MOFs) for another 24 h. For operation convenience in the cell experiments, the essential oil samples were measured in volume concentration *i.e*., "μL/mL". The mass of LEO can be calculated by its volume multiplied by its density (0.85 g/mL). The actual concentrations of LEO/β-CD and LEO/K-βCD-MOFs in all experiments were ten-fold of LEO, as the mass optimum core/wall ratio was 1:10. However, to enable further comparisons, the concentrations of these three were all expressed in "μL/mL, LEO equivalence". Different concentrations of the LEO were dissolved in different concentrations of DMSO, *i.e*., 0.001, 0.01 and 0.1 μL/mL in 0% DMSO, 0.2 μL/mL in 2% DMSO, 0.4 μL/mL in 4% DMSO, 0.5 μL/mL in 5% DMSO, 1 μL/mL in 10% DMSO, 2 μL/mL in 20% DMSO, respectively. For LEO/β-CD, 0.001–1 μL/mL were dissolved in 0% DMSO, and 2 μL/mL was dissolved in 2% DMSO. LEO/K-βCD-MOFs were directly dissolved in the medium. Therefore, the corresponding concentrations of DMSO were used as solvent controls for the cell viability and intracellular antioxidant activity experiments. The control was added with the growth medium instead of the samples. After PBS washing again, 5 mg/mL of MTT was added for another 4-h incubation. Subsequently, 150 μL of DMSO was added to dissolve the crystals, and the absorbance was then measured at 570 nm.

In the intracellular antioxidant activity experiment, HeLa cells were transferred and incubated according to the same procedures in cell viability assay. An aliquot of 100 μL of 20 μM DCFH-DA was mixed with 100 μL of 0.1 μL/mL of the LEO or included LEO (LEO/β-CD and LEO/K-βCD-MOFs) solution for 1 h. After the wells were washed by PBS (pH=7.4), 100 μL of 200 μM H_2O_2 was added into each well. The fluorescence intensities were measured every 5 min during the 1-h incubation time, and the integral area of the relative fluorescence intensity was calculated and marked as ∫SA. The excitation and emission wavelengths were 525 and 488 nm, respectively. When the growth medium was added instead of the samples, the integral area of the relative fluorescence intensity was ∫CA. The blank was prepared without both the samples and H_2O_2 solution. The intracellular antioxidant activity (CAA) was calculated according to the following equation:

$$\text{CAA (\%)} = 100 - (\int SA/\int CA) \times 100$$

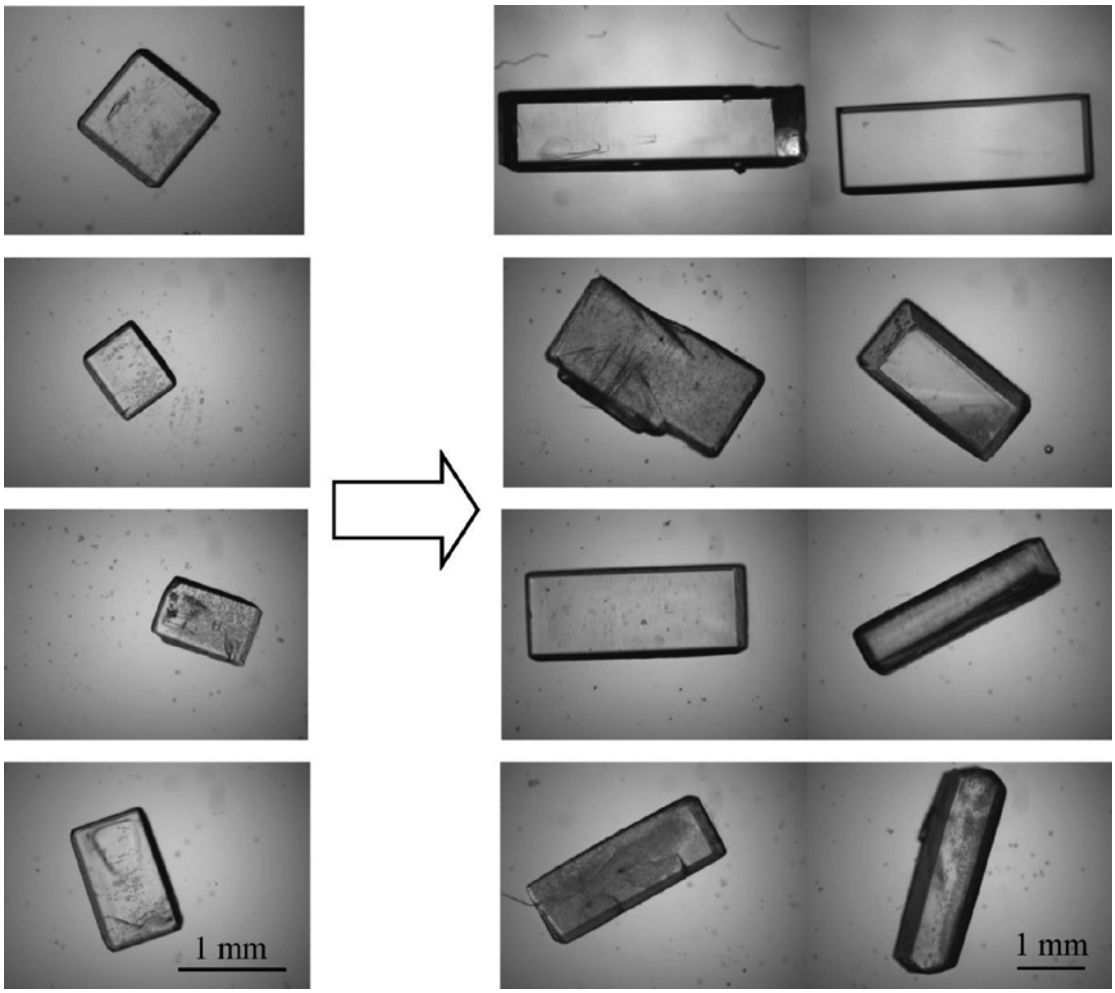

FIGURE 1. Optical microscope pictures of purified β-CD and metal-organic frameworks based on β-cyclodextrin and potassium cation (K-βCD-MOFs, magnification is 40 times).

Fourier transform infrared spectroscopy (FTIR)

The LEO, LEO/β-CD and LEO/K-βCD-MOFs inclusion, as well as the physical mixture of LEO and K-βCD--MOFs were analyzed by FTIR, which was conducted by KBr direct compression method, *i.e*., 1 mg of the sample was ground together with KBr (about 100 mg) into a fine powder, and compressed into the holder using a compression gauge. The liquid LEO was given a drop on the surface of KBr. The inclusion complexes were cleaned with petroleum ether 3 times to ensure no presence of LEO on the surface. The spectra were scanned within the wavelength 4,000 to 450 cm^{-1}. The number of scans and spectral resolution were 5 scans and 4 cm^{-1}, respectively.

Scanning electron microscope (SEM)

Besides the microscope observations, the morphological characterization of K-βCD-MOFs and LEO/K-βCD-MOFs was further carried out by SEM analysis. Material particles were fixed on the silicon wafer and sprayed with a 100 nm-thick gold. The microstructures of the samples, such as the shapes and surface characteristics, were then observed and photographed using the SEM.

Statistical analyses

The inclusion rates of LEO to β-CD or K-βCD-MOFs in the inclusion complexes were compared among the different mass core/wall ratios by one-way ANOVA, followed by a post--hoc multiple comparison (Tukey's Test). One-way ANOVA was also performed to compare the differences among LEO, LEO/β-CD and LEO/K-βCD-MOFs at the same concentration (concentrations of the two including LEO were expressed as LEO equivalence) in thermal and pH stabilities, cell viabilities, as well as CAA. All statistical analyses were performed using the Statistical Package for Social Science (SPSS) version 16.0. Three replicates with mean values and standard deviations were carried out for all statistical analyses.

RESULTS AND DISCUSSION

Formation of K-βCD-MOFs

The K-βCD-MOFs were produced from the purified β-CD by the methanol diffusion method. The morphology features of their crystal structures were compared using an optical microscope (×40) and shown in Figure 1. They were both relatively regular and transparent with a neat appear-

ance. The β-CD showed shorter rectangular shape, while the K-βCD-MOFs were larger and longer.

Formation of LEO/β-CD and LEO/K-βCD-MOFs inclusion complexes

Based on the formation of the wall material K-βCD--MOFs, LEO was microencapsulated as the core to produce inclusion complexes in different mass core/wall ratios. The inclusion rates of LEO/K-βCD-MOFs were shown in Figure 2. The inclusion rate increased significantly with the increase of the ratio, *i.e.*, with the increasing mass of wall material (K-βCD-MOFs), the inclusion rate of LEO to the wall significantly increased. The inclusion rate reached up to 93.45% with the core/wall ratio of 1:10, while no significant changes were observed for the rate of 95.67% with ratio of 1:12. Therefore, to save the resource and energy, the mass core/wall ratio of 1:10 was used for the future formation of LEO/K-βCD-MOFs complexes. In addition, the inclusion rates of LEO to K-βCD--MOFs and β-CD were also compared with the ratio of 1:10. The latter was only 78.42%, which was significantly lower than the rate of LEO/K-βCD-MOFs with the same ratio.

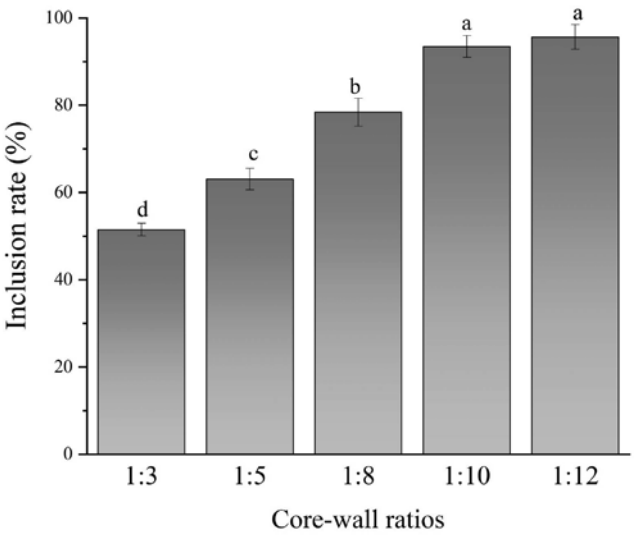

FIGURE 2. The inclusion rate of lavender essential oil (LEO) to metal-organic frameworks based on β-cyclodextrin and potassium cation (K-βCD-MOFs) under different core/wall ratios.

Bars with different lower-case letters show significant differences of inclusion rate among different core/wall ratios at p≤0.05 according to one-way ANOVA test. Data are reported as the mean ± SD of three replicates.

Properties of LEO, LEO/β-CD and LEO/K-βCD-MOFs

Thermal stability

The changes of LEO, LEO/β-CD and LEO/K-βCD--MOFs inclusion complexes under heat treatment at 90°C were studied during 10-day period with 1-day interval. After 24-h heat treatment, the preservation rate of LEO decreased to 53.27%, while the rate of LEO in the LEO/K-βCD-MOFs complex still remained at 90.13% (Figure 3A). As the heating time went on, the preservation rate of LEO and its inclusion complexes kept a gradually decreasing trend, with LEO's rate decreasing more rapidly and significantly than those of the complexes (Figure 3A). After 10 days, the preservation rate of LEO/K-βCD-MOFs and LEO/β-CD remained at 66.88 and 31.50%, respectively, while the rate of LEO was only 18.00% in the same environment (Figure 3A). The thermal stability of LEO could be significantly improved by embedding with β-CD and K-βCD-MOFs, especially the latter. These phenomena suggested that K-βCD-MOFs could provide better pro-

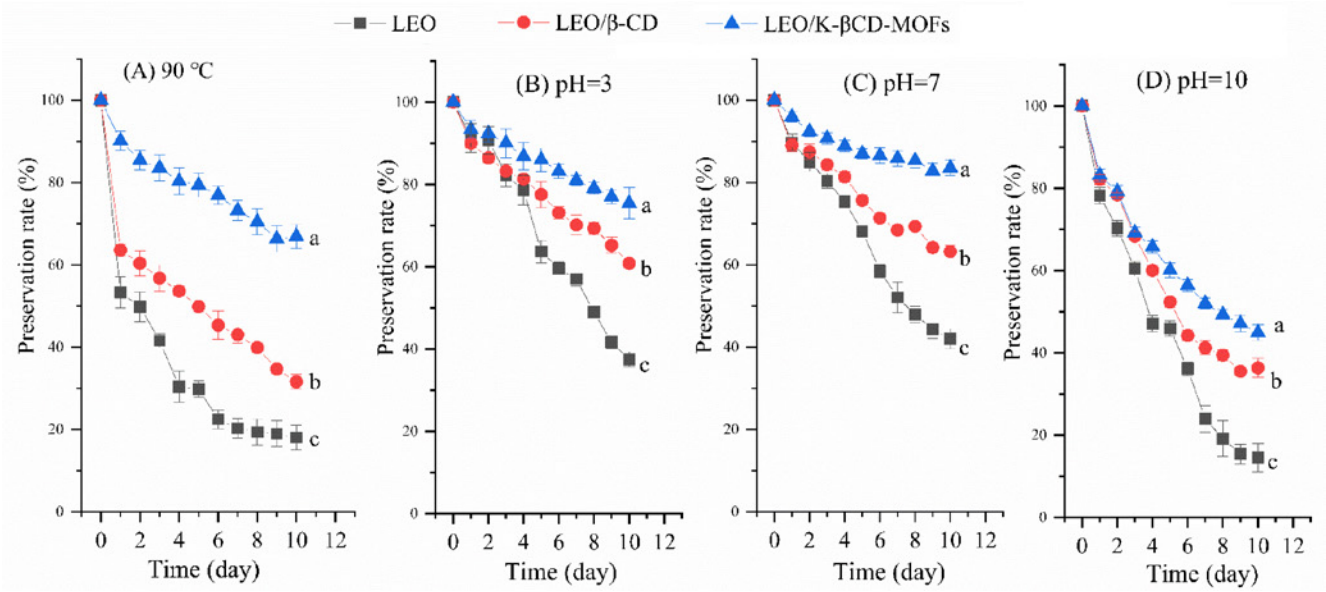

FIGURE 3. Thermal- (A) and pH-stabilities (B, C and D) of lavender essential oil (LEO), LEO/β-cyclodextrins (LEO/β-CD) and LEO/ metal-organic frameworks based on β-cyclodextrin and potassium cation (LEO/K-βCD-MOFs) inclusion complexes.

The LEO/β-CD and LEO/K-βCD-MOFs inclusion complexes with core/wall ratio of 1:10 were used. Lines with different lower-case letters show significant differences of preservation rate at day 10 among LEO, LEO/β-CD and LEO/K-βCD-MOFs under the same conditions at p≤0.05 according to one-way ANOVA test. Data are reported as the mean ± SD of three replicates.

tection for LEO than β-CD against evaporation/degradation after LEOs were embedded. This could be explained by the improved thermal stability of both LEO and β-CD rendered by K-βCD-MOFs. Han *et al*. [2018] reported that the structures of CDs were modified, and the CD-MOFs were more thermally stable in an aqueous medium or in the physiological environment, as well as showed preferable solubility in water. Lv *et al*. [2017] reported that sucralose degraded very fast at 90°C for only one hour with about 14% left, while the stability of sucralose was dramatically enhanced by CD-MOFs, with only 13.7% decomposition under the same heat environment within 24 h. Furthermore, for future and better applications of LEO, the thermal stabilities of the inclusion complexes under many other thermal conditions and different working temperature (*e.g*., 50, 75, 100 and 121°C) should be studied.

pH stability

The results of the influence of different pH values (3, 7 and 10) on the stabilities of LEO, LEO/β-CD and LEO/β-CD-MOFs were obtained during 10-day period, and the variation trends of the preservation rate were shown in Figure 3B, C, D. Under acidic and neutral conditions, the stabilities of LEO and its inclusion complexes were better than under alkali condition, and the acid resistance of LEO/β-CD and LEO/β-CD-MOFs was much stronger than that of LEO itself (Figure. 3B, C). In strong alkali environment, the stabilities of LEO and LEO inclusion complexes decreased sharply. However, the stabilities of these complexes were still stronger than that of non-included LEO (Figure 3D). Therefore, in general, LEO/β-CD and LEO/β-CD-MOFs exhibited better acid-alkali resistance stabilities than the original oil, with better applicability under neutral and acidic conditions. This result can be attributed to the fact that the essential oils are always stable in weak acidic to neutral environment and are often applied in acidic conditions [Bensouda *et al*., 2019; Wang *et al*., 2009].

Intracellular antioxidant activities

Reduction reaction of MTT occurs with the presence of succinodehydrogenase in living cells, and MTT changes from yellow tetrazolium salt to purple formazan. Therefore, the absorbance at the maximum absorption wavelength of 570 nm of the purple product could indirectly reflect the amount of the living cells [Adach *et al*., 2016]. The effects of the different concentrations of LEO, LEO/β-CD and LEO/K-βCD-MOFs on the cell viabilities of HeLa cells were analyzed (Figure 4). Within the concentration range from 0.001 to 0.2 μL/mL, no significant difference was found among LEO, LEO/β-CD and LEO/K-βCD-MOFs. Both LEO and its inclusion complexes did not pose negative effects on the HeLa cell viabilities with concentrations lower than 0.2 μL/mL. However, the HeLa cell viabilities decreased with the concentration higher than 0.4 μL/mL. The inhibitory effects on cell viabilities of LEO/K-βCD-MOFs were significantly higher than those of LEO at concentration 0.4, 0.5 and 1 μL/mL, and also significantly higher than LEO/β-CD at 0.5 μL/mL. All the samples showed similar inhibitions on HeLa cells with the highest concentration at 2 μL/mL. The growth and viabilities of HeLa cells were inhibited, indicating the lavender essential oil could play an anticancer role with the concentrations reaching up to 0.4 μL/mL. Previous studies showed potential anticancer and antiproliferative activities of LEO by the induction of apoptosis and necrosis of cancer cells [Gezici, 2018]. LEO also exhibited on antitumor effects on the human prostate cancer, and its antitumor effect was associated with cell proliferation inhibition and apoptosis induction in xenograft tumors [Zhao *et al*., 2017]. Besides, the components of LEO also showed anticancer and antitumor effects. For example, one constituent of lavender oil – perillyl alcohol – has recently been identified as a potential anticancer agent, which may be useful in both treatment and prevention [Liston *et al*., 2003; Samaila *et al*., 2004]. Linalool and linalyl acetate also showed strong inhibitory effects on human prostate cancer PC-3 and DU145 cells [Zhao *et al*., 2017]. Usta *et al*. [2009] reported that linalool could decrease the viability of HepG20 to 50% and 0% by concentrations of 4 μM and 2 μM, respectively. Differences in the inhibitory activity of LEO and its microcapsules were in the order LEO/β-CD-MOFs > LEO/β-CD > LEO, and could be easily ascribed to the higher solubility of β-CD-MOFs than β-CD [Han *et al*., 2018], as well as the higher solubility of the complexes than LEO itself. All these related to the potential applications of LEO as potential anticancer/antitumor agents deserve further researches. Besides the anticancer role of LEO in killing HeLa cells, in the present study we focused on whether the intracellular antioxidant activities of LEO could be improved by microencapsulation by K-βCD-MOFs.

Although the chemical methods used to evaluate antioxidant activities *in vitro* are easy, convenient and inexpensive, they could reflect neither the antioxidant activities of the anti-

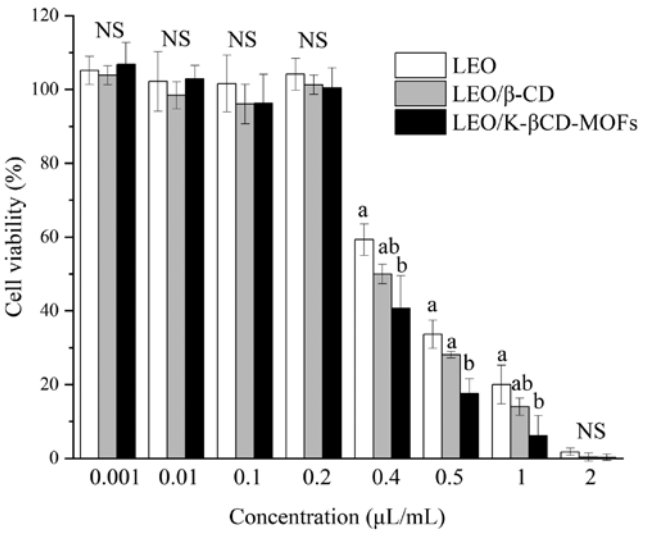

FIGURE 4. Effects of lavender essential oil (LEO), LEO/β-cyclodextrins (LEO/β-CD) and LEO/ metal-organic frameworks based on β-cyclodextrin and potassium cation (LEO/K-βCD-MOFs) inclusion complexes on cell viability in HeLa cells.

The LEO/β-CD and LEO/K-βCD-MOFs inclusion complexes with core/wall ratio of 1:10 were used. Bars with different lower-case letters show significant differences among the effects of LEO, LEO/β-CD and LEO/K-βCD-MOFs on cell viability at $p \leq 0.05$ according to one-way ANOVA test. NS: Not significant difference. Data are reported as the mean ± SD of three replicates.

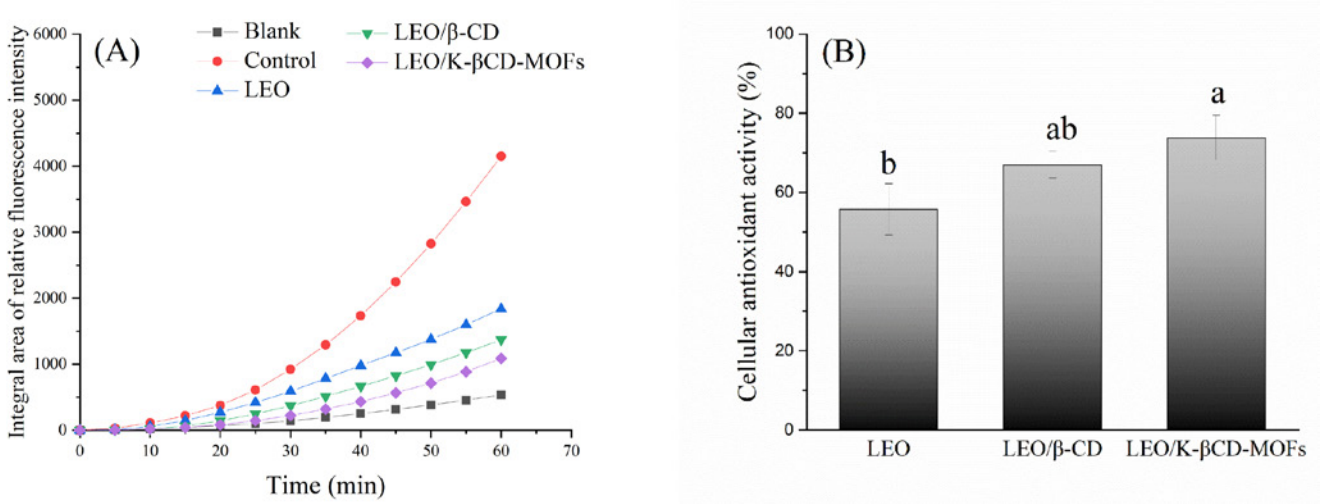

FIGURE 5. The integral areas of relative fluorescence intensity (A) and the intracellular antioxidant activity (CAA) of lavender essential oil (LEO), LEO/β-cyclodextrins (LEO/β-CD) and LEO/ metal-organic frameworks based on β-cyclodextrin and potassium cation (LEO/K-βCD-MOFs) (B) in HeLa cells.

The LEO/β-CD and LEO/K-βCD-MOFs inclusion complexes with core/wall ratio of 1:10 were used. Bars with lower-case letters show significant differences among LEO, LEO/β-CD and LEO/K-βCD-MOFs at $p \leq 0.05$ according to one-way ANOVA. Data are reported as the mean ± SD of three replicates.

oxidants *in vivo* nor the real physiological environment of the human body. On the other hand, animal models or even human experiments are relatively expensive and time-consuming. Cell model could predict the antioxidant capacities of the antioxidants in the human body more accurately than chemical methods. Therefore, the cell model method is a good choice to simulate the internal physiological environment of the human body, study the intracellular antioxidant activities, and provide an economical and rapid method for better antioxidant research. Consequently, HeLa cells were chosen to simulate an *in vivo* environment to investigate the intracellular antioxidant activities of the LEO and its inclusion complexes with the concentration of 0.1 μL/mL, which was within the non-cytotoxic range (<0.2 μL/mL). In the living cells, non-fluorescent DCFH-DA could be hydrolyzed by esterases with the production of 2',7'-dichlorodihydrofluorescein (DCFH) [Labieniec & Gabryelak, 2007]. The non-fluorescent DCFH are then oxidized to fluorescent product 2',7'-dichlorofluorescein (DCF) by reactive oxygen species (ROS), which could be induced by H_2O_2. The fluorescent intensity of DCF correlates with the cellular ROS content, and this intensity decreases with the presence of antioxidants due to their ability to scavenge free radicals [Qian *et al*., 2012; Xu & Chang, 2012].

Figure 5A shows the integral areas of relative fluorescence intensity of HeLa cells (control) and HeLa cells with LEO and microcapsules of LEO/β-CD and LEO/ K-βCD-MOFs. After 1-h H_2O_2 stimulation, the intensity in the control was about 8 times as that of the blank without H_2O_2 stimulation. The relative fluorescence intensities of cells with LEO, LEO/β-CD and LEO/K-βCD-MOFs were all significantly lower than the control, indicating that both LEO and its inclusion complexes showed significant intracellular ROS scavenging activity in HeLa cells. The intracellular antioxidant activity (CAA) of LEO and its inclusion complexes were also shown in Figure 5B. LEO/K-βCD-MOFs showed significantly higher CAA than LEO. The lavender essential oil has been reported with high contents of oxygenated monoterpenes (31.53%) and monoterpene hydrocarbons (8.03%) [Dong *et al.*, 2020]. For example, linalool – which is the major oxygenated monoterpene of lavender – accounts for 19.71% of its essential oil [Dong *et al*., 2020]. The essential oils rich in monoterpenes and oxygenated monoterpenes generally show a high antioxidative potential [Deba *et al*., 2008; Tepe *et al*., 2004]. Monoterpenes are very active due to the presence of a double bond between two carbon atoms (C=C), and thus they could act as free radical scavengers [Mercier *et al*., 2009]. Therefore, lavender essential oil played a role in scavenging intracellular ROS, leading to the high CAA of LEO and its microencapsulated products.

The higher scavenging ability of LEO/K-βCD-MOFs is due to the higher solubility and availability in the cells compared to LEO and LEO/β-CD, which is in agreement with the reported higher solubility of K-βCD-MOFs than β-CD [Han *et al*., 2018]. Another possible reason might be the different microencapsulation capabilities of K-βCD-MOFs for different guest molecules. Yuan *et al*. [2019] reported that the microencapsulation by HPCD could change the relative contents of the major components of LEO dramatically. For example, contents of linalyl anthranilate and linalool changed from 42.18% to 24.05% and 34.94% to 60.87%, respectively, *i.e.*, they found that hydrocarbons and esters decreased, while conversely, carbonyl compounds and alcohols increased. Alcohols and carbonyl compounds were easier encapsulated by HPCD than other compounds of LEO. This phenomenon might be attributed to the properties of the hydrophobic cavity of HPCD [Yuan *et al*., 2019]. The similar explanation might apply to the present study. Therefore, future study should be carried on to analyze the LEO composition before and after microencapsulation by K-βCD-MOFs, and also to compare antioxidant activities among different compounds in LEO.

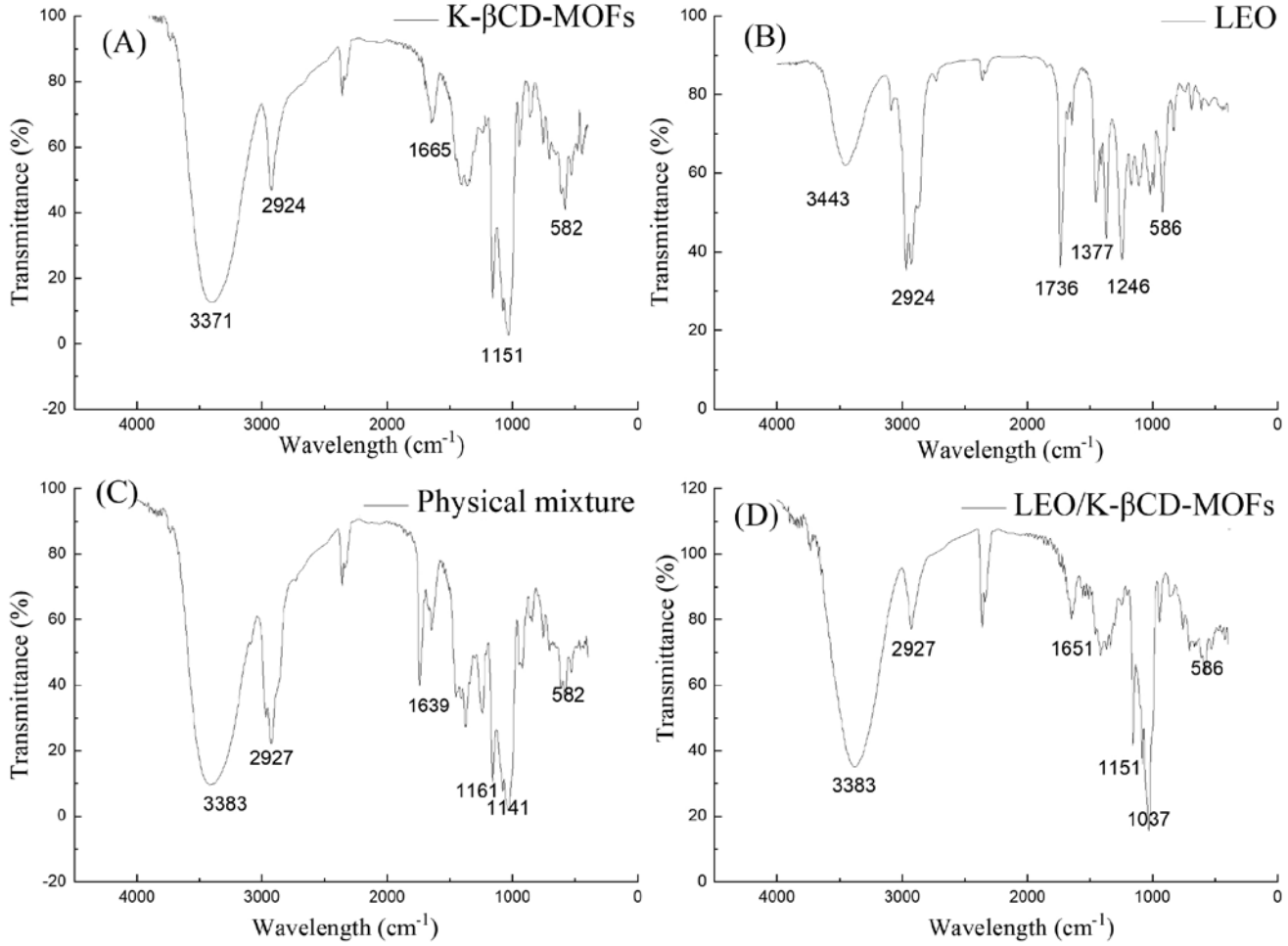

FIGURE 6. Infrared spectra of metal-organic frameworks based on β-cyclodextrin and potassium cation (K-βCD-MOFs) (A), lavender essential oil (LEO) (B), physical mixture of LEO and K-βCD-MOFs(C), and LEO/K-βCD-MOFs inclusion complex (D).

The LEO/β-CD and LEO/K-βCD-MOFs inclusion complexes with core/wall ratio of 1:10 were used.

Wu *et al*. [2019] synthesized porous Zn@MOF and used it for microencapsulation of thymol for pathogen inhibition, and the T-Zn@MOF was proved to effectively inhibit *E. coli*. The present study was successful in synthesizing edible MOFs using β-CD and potassium ion. It is hopeful that K-βCD-MOFs could be applied to the applications of LEO with improved antioxidant activities in the food industries in the near future.

Characterization of LEO, LEO/β-CD and LEO/K-βCD--MOFs

Fourier transform infrared spectroscopy (FTIR)

The Fourier transform infrared spectroscopy technology is usually helpful in detecting the interaction between cyclodextrin or MOFs as host and the guest molecules [Liu *et al*., 2019; Tu *et al*., 2020; Yuan *et al*., 2019]. The inclusion complexes could be confirmed by FTIR with the variation of position, intensity and even the shape of the peaks [Yuan *et al*., 2019]. Yuan *et al*. [2019] employed FTIR to provide the solid evidence for the formation of inclusion compounds of LEO by HPCD. Tu *et al*. [2020] also applied FTIR to support the formation of an inclusion complex of Mxene/carbon nanohorn with K-βCD-MOFs. FTIR was also applied to demonstrate the formation of inclusion complex in the present study. The infrared spectra of the K-βCD-MOFs, LEO, the physical mixture of LEO and K-βCD-MOFs, as well as LEO/K-βCD--MOFs inclusion complex were shown in Figure 6. Because the inclusion complexes were cleaned with petroleum ether 3 times, it could be considered that no LEO existed on the surface of the inclusion complex. If the absorption peak of the functional group of LEO could be found in the infrared absorption spectrogram of the inclusion complexes, we can deduce that LEO has been encapsulated by K-βCD-MOFs.

The spectrum of K-βCD-MOFs (Figure 6A) showed the characteristic absorption peaks of β-CD, suggesting the synthetic K-βCD-MOFs based on β-CD still kept the cavity structure of β-CD. The absorption peak between 3300–3400 cm^{-1} belongs to –OH, and the characteristic peak of $–CH_2$ is at 2924 cm^{-1}. The peaks around 1151 cm^{-1} represent the C–O stretching vibration absorption peak of K-βCD-MOFs and the inner cavity of the inclusion complexes.

Figure 6B showed the LEO infrared spectrum with the characteristic absorption peak of C=O at 1651 cm^{-1}. The spec-

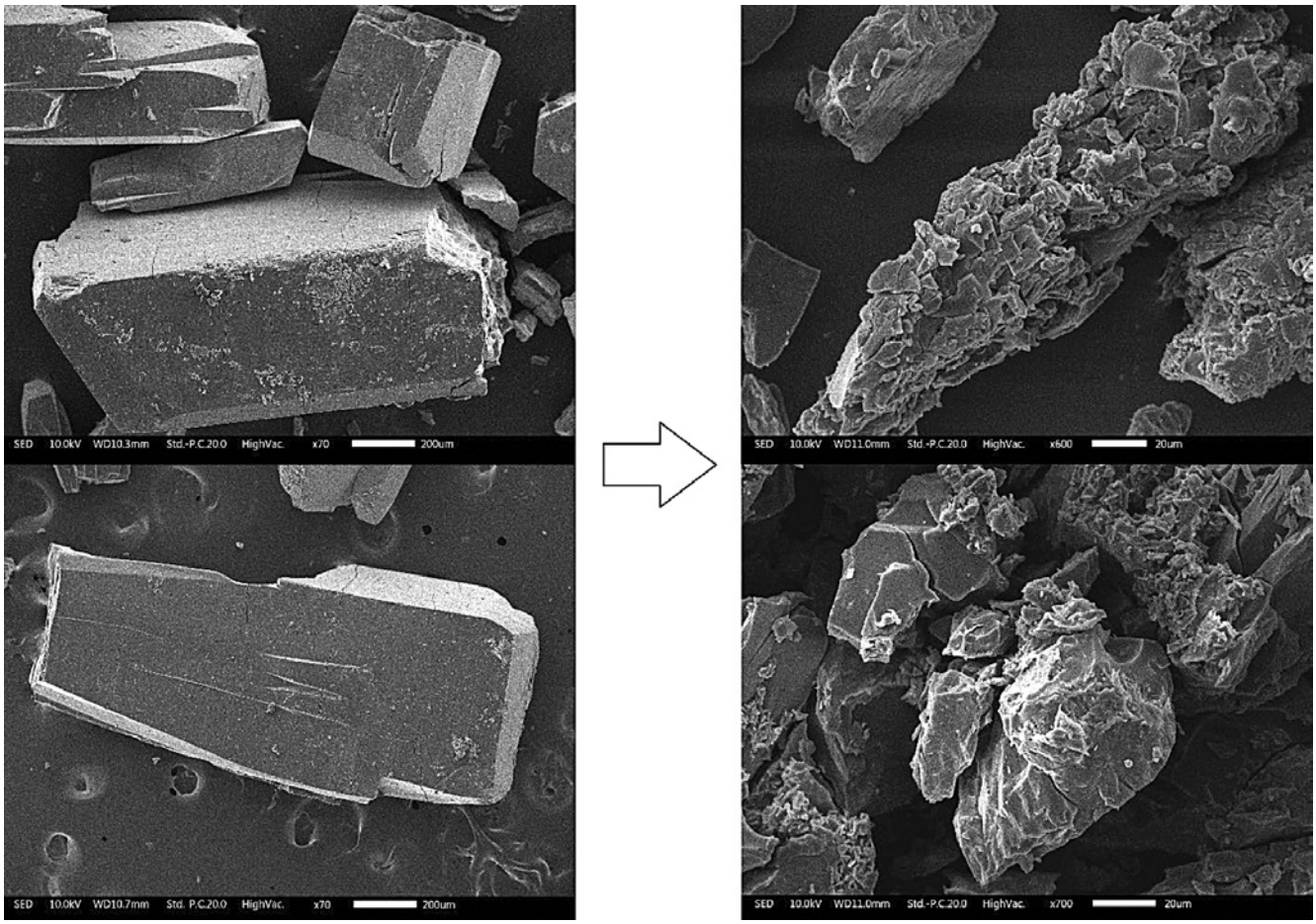

β-CD-MOFs **LEO/K-βCD-MOFs**

FIGURE 7. Scanning electron microscope pictures of metal-organic frameworks based on β-cyclodextrin and potassium cation (K-βCD-MOFs) and lavender essential oil (LEO)/K-βCD-MOFs inclusion complex.

The LEO/K-βCD-MOFs inclusion complexes with core/wall ratio of 1:10 were used. The magnifications are 70 and 700 times, respectively.

tra of the physical mixture and the inclusion complex were presented in Figure 6C, D, respectively. The main absorption peaks (–OH, C=O, C–O, $–CH_3$ and $–CH_2$) of the two substances were generally similar to those of K-βCD-MOFs. As the mass core/wall ratio was 1:10, the amounts of K-βCD-MOFs in both substances were much larger than that of LEO, resulting in the embedment of the LEO peaks in the bulk K-βCD-MOFs matrix. As the microencapsulation of LEO by K-βCD-MOFs was probably due to van der Waals force [Li *et al*., 2017], the absorption frequency and peak shape in the infrared spectra of the functional groups did not change after the microencapsulation. However, the peak intensities of the inclusion complexes were different from those of K-βCD-MOFs and LEO. This could be explained by the fact that LEO was bound and affected by the van der Waals force, which might cause the hinderance of its vibration and finally lead to the changes of intensity or even the disappearance of the peaks.

Finally, the spectrum of the inclusion compounds was obviously different from that of the physical mixture, especially regarding the C=O stretching vibration peak (around 1651 cm^{-1}) of LEO. This indicated that the LEO's environment in the inclusion compounds was different from that in the physical mixture. The weakening and the disappearance of some absorption peaks suggested that LEO has been successfully loaded as some groups have entered the cavity of CD. All the above infrared results proved the formation of LEO/K-βCD-MOFs.

Scanning electron microscope (SEM)

SEM has been commonly used to characterize the morphology and crystal structures of different MOFs [Wu *et al*., 2019]. To further characterize the inclusion complexes, the microstructures of K-βCD-MOFs and LEO/K-βCD-MOFs were observed by SEM. First, the representative SEM images of K-βCD-MOFs were shown in Figure 7. The crystalline K-βCD-MOFs has a long cuboid morphology, which is consistent with other researches [Liu *et al*., 2019; Tu *et al*., 2010]. The present study and the previous researches indicated K-βCD-MOFs were a rectangular solid with various sizes from millimeter to micron. For instance, Liu *et al*. [2019] showed the size of K-βCD-MOFs varied from 500 nm to 2 or several millimeters once examined by transmission electron microscope (TEM) and SEM. Figure 1 shows the size of K-βCD-MOFs was around several millimeters. Besides, by comparison with Figure 7, K-βCD-MOFs could be deemed smooth and long cubic crystals, while LEO/K-βCD-MOFs exhibited a relatively rough surface, which is a new image.

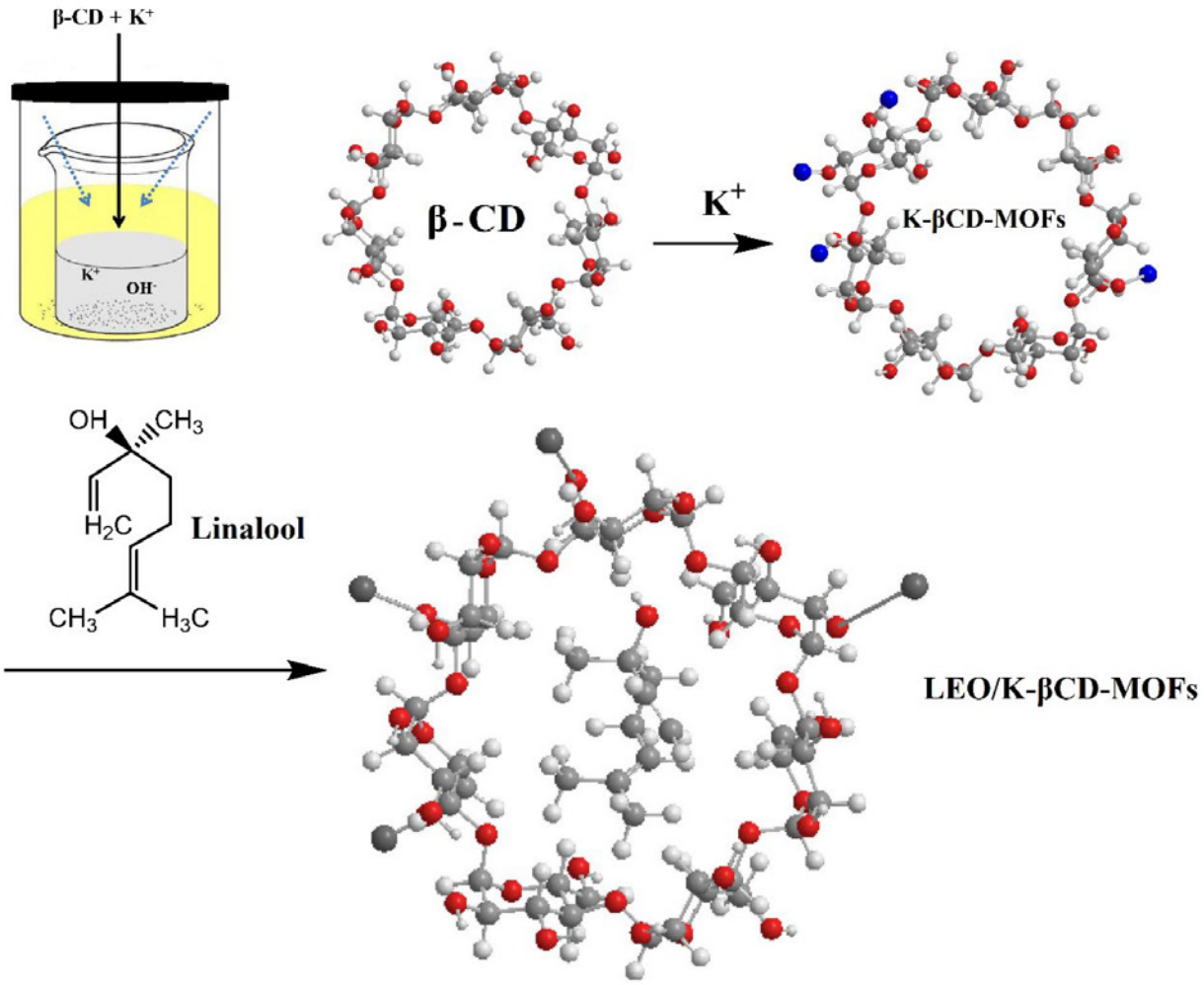

FIGURE 8. The scheme for the possible microencapsulation mechanism of lavender essential oil (LEO) by metal-organic frameworks based on β-cyclodextrin and potassium cation (K-βCD-MOFs) as the inclusion materials.

Linalool as the main component of LEO was taken as an example.

Possible mechanism of the production of LEO/K-βCD--MOFs microcapsule

The formation of K-βCD-MOFs was plotted in Figure 8. The potassium ion (K^+) is paired with seven oxygen atoms (O) of the four surrounding β-CD [Lu *et al*., 2015]. On the other hand, to further deduce the microencapsulation mechanism of the production of LEO/K-βCD-MOFs microcapsule, linalool is taken as an example as it is the main component of LEO [Dong *et al*., 2020]. The optimum mass core/wall ratio of linalool to K-βCD-MOFs at 1:10 is equaled to the molar ratio of about 1:1. The scheme for the possible microcapsule formation is shown in Figure 8. In detail, when linalool was encapsulated by K-βCD-MOFs, one K-βCD-MOFs molecules could encapsulate one linalool molecule (Figure 8). The specific reaction mechanism of the microencapsulation between LEO and K-βCD-MOFs deserves further research by single crystal X-ray diffraction, elemental analysis, and so forth.

CONCLUSIONS

Studies on the microencapsulation of lavender essential oil by β-CD and K-βCD-MOFs as well as analyses of the stability and antioxidant activity in HeLa cells of the LEO/β-CD and LEO/K-βCD-MOFs inclusion complexes were carried out. Our results showed the formation of a complex between LEO and CD-MOFs, as evidenced by FTIR and SEM. Furthermore, the microcapsules of LEO/K-βCD-MOFs were proved to be more thermally and acid-base stable than LEO, and its intracellular antioxidant effect was also significantly improved by encapsulation. The microencapsulation of LEO by K-βCD-MOFs not only did not inhibit the intracellular antioxidant activities of LEO, but also significantly improved their ROS scavenging abilities. All these indicated the application of lavender essential oil to food and medicine would be expanded, as the new functional K-βCD-MOFs materials prepared based on β-CD have great benefits to future. This information provides solid evidence and foundation for the future applications of LEO, and thus improves the production of tailor-made commodities by addressing different requirements of manufacturers of this herbal plant as medicines, herbal teas, food seasoning, cosmetics, and *etc*. The advantages of K-βCD-MOFs make them not only limited to chemical industry, but also applicable to new fields including foods, pharmaceuticals or health care products, *etc*.

RESEARCH FUNDING

The present work was supported by the Natural Science Foundation of Tianjin (grant numbers 17JCQNJC02400 and 18JCYBJC96000), the National Training Programs for Innovation and Entrepreneurship of Undergraduates (grant number 201910069019), 131 Second Level Innovative Talents Training Project in Tianjin, and Young and Middle-aged Key Innovative Talents Training Project of Tianjin Universities.

CONFLICT OF INTEREST

Authors declare no conflict of interest

ORCID IDs

J. Tan http://orcid.org/0000-0002-3515-7804
Y. Wang https://orcid.org/0000-0002-4933-9158

REFERENCES

1. Abuçafy, M.P., Caetano, B.L., Chiari-Andréo, B.G., Fonseca-Santos, B., do Santos, A.M., Chorilli, M., Chiavacci, L.A. (2018). Supramolecular cyclodextrin-based metal-organic frameworks as efficient carrier for anti-inflammatory drugs. *European Journal of Pharmaceutics and Biopharmaceutics, 127*, 112–119. https://doi.org/10.1016/j.ejpb.2018.02.009
2. Adach, K., Fijalkowski, M., Gajek, G., Skolimowski, J., Kontek, R., Blaszczyk, A. (2016). Studies on the cytotoxicity of diamond nanoparticles against human cancer cells and lymphocytes. *Chemico-biological Interactions*, 254, 156–166. https://doi.org/10.1016/j.cbi.2016.06.004
3. Bensouda, Z., Sfaira, M., Touhami, M.E., Farah, A., Hammouti, B. (2019). Extraction, characterization and anticorrosion potential of an essential oil from orange zest as eco-friendly inhibitor for mild steel in acidic solution. *Journal of Bio-and Tribo-Corrosion, 5*(4), 84. https://doi.org/10.1007/s40735-019-0276-y
4. Cavanagh, H.M., Wilkinson, J.M. (2005). Lavender essential oil: A review. *Australian Infection Control*, *10*(1), 35–37. https://doi.org/10.1071/HI05035
5. Deba, F., Xuan, T.D., Yasuda, M., Tawata, S. (2008). Chemical composition and antioxidant, antibacterial and antifungal activities of the essential oils from *Bidens pilosa* Linn. var. *Radiata. Food Control, 19*(4), 346–352. https://doi.org/10.1016/j.foodcont.2007.04.011
6. Deng, S., Liu, H., Qi, C., Yang, A., Li, Z. (2018). Study on preparation and inclusion behavior of inclusion complexes between β-cyclodextrin derivatives with benzophenone. *Journal of Inclusion Phenomena and Macrocyclic Chemistry, 90*(3–4), 321–329. https://doi.org/10.1007/s10847-018-0787-z
7. Dong, G., Bai, X., Aimila, A., Aisa, H.A., Maiwulanjiang, M. (2020). Study on lavender essential oil chemical compositions by GC-MS and improved pGC. *Molecules*, *25*(14), 3166. https://doi.org/10.3390/molecules25143166
8. Gezici, S. (2018). Promising anticancer activity of lavender (*Lavandula angustifolia* Mill.) essential oil through induction of both apoptosis and necrosis. *Annals of Phytomedicine, 7*(2), 38–45. https://doi.org/10.21276/ap.2018.7.2.5
9. Han, Y., Liu, W., Huang, J., Qiu, S., Zhong, H., Liu, D., Liu, J. (2018). Cyclodextrin-based metal-organic frameworks (CD-MOFs) in pharmaceutics and biomedicine. *Pharmaceutics, 10*(4), 271. https://doi.org/10.3390/pharmaceutics10040271
10. Insawang, S., Pripdeevech, P., Tanapichatsakul, C., Khruengsai, S., Monggoot, S., Nakham, T., Artrod, A., D'Souza, P.E., Panuwet, P. (2019). Essential oil compositions and antibacterial and antioxidant activities of five Lavandula *stoechas* cultivars grown in Thailand. *Chemistry & Biodiversity, 16*(10), e1900371. https://doi.org/10.1002/cbdv.201900371
11. Kumar, S., Jain, S., Nehra, M., Dilbaghi, N., Marrazza, G., Kim, K.H. (2020). Green synthesis of metal-organic frameworks: A state-of-the-art review of potential environmental and medical applications. *Coordination Chemistry Reviews, 420*, 213407. https://doi.org/10.1016/j.ccr.2020.213407
12. Kwiatkowski, P., Łopusiewicz, Ł., Kostek, M., Drozłowska, E., Pruss, A., Wojciuk, B., Sienkiewicz, M., Zielińska-Bliźniewska, H., Dołęgowska, B. (2020). The antibacterial activity of lavender essential oil alone and in combination with octenidine dihydrochloride against MRSA strains. *Molecules, 25*(1), 95. https://doi.org/10.3390/molecules25010095
13. Labieniec, M., Gabryelak, T. (2007). Antioxidative and oxidative changes in the digestive gland cells of freshwater mussels *Unio tumidus* caused by selected phenolic compounds in the presence of H_2O_2 or Cu^{2+} ions. *Toxicology in Vitro, 21*(1), 146–156. https://doi.org/10.1016/j.tiv.2006.09.017
14. Li, S., Huo, F. (2015). Metal-organic framework composites: from fundamentals to applications. *Nanoscale, 7*(17), 7482–7501. https://doi.org/10.1039/C5NR00518C
15. Li, X., Guo, T., Lachmanski, L., Manoli, F., Menendez-Miranda, M., Manet, I., Guo, Z., Wu, L., Zhang, J.W., Gref, R. (2017). Cyclodextrin-based metal-organic frameworks particles as efficient carriers for lansoprazole: study of morphology and chemical composition of individual particles. *International Journal of Pharmaceutics, 531*(2), 424–432. https://doi.org/10.1016/j.ijpharm.2017.05.056
16. Lis-Balchin, M. (2002). Lavender: The Genus *Lavandula*. (Medicinal and Aromatic Plants – Industrial Profiles). 1st ed., Taylor & Francis, London, UK, p. 86, p. 100. https://doi.org/10.1201/9780203216521
17. Liston, B.W., Nines, R., Carlton, P.S., Gupta, A., Aziz, R., Frankel, W., Stoner, G.D. (2003). Perillyl alcohol as a chemopreventive agent in N-nitrosomethylbenzylamine-induced rat esophageal tumorigenesis. *Cancer Research, 63*(10), 2399–2403.
18. Liu, C., Wang, P., Liu, X., Yi, X., Zhou, Z., Liu, D. (2019). Multifunctional β-cyclodextrin MOF-derived porous carbon as efficient herbicides adsorbent and potassium fertilizer. *ACS Sustainable Chemistry & Engineering, 7*(17), 14479–14489. https://doi.org/10.1021/acssuschemeng.9b01911
19. Liu, J., Bao, T.Y., Yang, X.Y., Zhu, P.P., Wu, L.H., Sha, J.Q., Zhang, L., Dong, L.Z., Cao, X.L., Lan, Y.Q. (2017). Controllable porosity conversion of metal-organic frameworks composed of natural ingredients for drug delivery. *Chemical Communications, 53*(55), 7804–7807. https://doi.org/10.1039/C7CC03673F
20. Lu, H.J., Yang, X.N., Sha, J.Q., Li, C.D., Li, X.T. (2015). Synthesis and AM inclusion technology of β-CD-metal organic framework. *Journal of Harbin University of Science and Technology, 20*(4), 35–40 (in Chinese; English abstract).

21. Lv, N., Guo, T., Liu, B., Wang, C., Singh, V., Xu, X., Li, X., Chen, D., Gref, R., Zhang, J. (2017). Improvement in thermal stability of sucralose by γ-cyclodextrin metal-organic frameworks. *Pharmaceutical Research, 34*(2), 269–278. https://doi.org/10.1007/s11095-016-2059-1
22. Mercier, B., Prost, J., Prost, M. (2009). The essential oil of turpentine and its major volatile fraction (α-and β-pinenes): A review. *International Journal of Occupational Medicine and Environmental Health, 22*(4), 331–342. https://doi.org/10.2478/v10001-009-0032-5
23. Michida, W., Ezaki, M., Sakuragi, M., Guan, G., Kusakabe, K. (2015). Crystal growth of cyclodextrin-based metal-organic framework with inclusion of ferulic acid. *Crystal Research and Technology, 50*(7), 556–559. https://doi.org/10.1002/crat.201500053
24. Partanen, R., Ahro, M., Hakala, M., Kallio, H., Forssell, P. (2002). Microencapsulation of caraway extract in β-cyclodextrin and modified starches. *European Food Research and Technology, 214*(3), 242–247. https://doi.org/10.1007/s00217-001-0446-1
25. Qian, Z.J., Kang, K.H., Kim, S.K. (2012). Isolation and antioxidant activity evaluation of two new phthalate derivatives from seahorse, *Hippocampus kuda* Bleeler. *Biotechnology and Bioprocess Engineering, 17*(5), 1031–1040. https://doi.org/10.1007/s12257-012-0115-1
26. Samaila, D., Ezekwudo, D.E., Yimam, K.K., Elegbede, J.A. (2004). Bioactive plant compounds inhibited the proliferation and induced apoptosis in human cancer cell lines, *in vitro*. *In Transactions of the Integrated Bio-Medical Informatics & Enabling Technologies Symposiums, 1*, 34–42.
27. Shafaei, S.M., Nourmohamadi-Moghadami, A., Kamgar, S. (2017). Experimental analysis and modeling of frictional behavior of lavender flowers (*Lavandula stoechas* L.). *Journal of Applied Research on Medicinal and Aromatic Plants, 4*, 5–11. https://doi.org/10.1016/j.jarmap.2016.07.001
28. Smaldone, R.A., Forgan, R.S., Furukawa, H., Gassensmith, J.J., Slawin, A.M., Yaghi, O.M., Stoddart, J.F. (2010). Metal-organic frameworks from edible natural products. *Angewandte Chemie International Edition, 49*(46), 8630–8634. https://doi.org/10.1002/anie.201002343
29. Tepe, B., Donmez, E., Unlu, M., Candan, F., Daferera, D., Vardar-Unlu, G., Sokmen, A. (2004). Antimicrobial and antioxidative activities of the essential oils and methanol extracts of *Salvia cryptantha* (Montbret et Aucher ex Benth.) and *Salvia multicaulis* (Vahl). *Food Chemistry, 84*(4), 519–525. https://doi.org/10.1016/S0308-8146(03)00267-X
30. Thombre, R.S., Kanekar, P.P., Rajwade, J.M. (2013). Production of cyclodextrin glycosyltransferase from alkaliphilic *Paenibacillus sp* L55 MCM B-1034 isolated from alkaline lonar lake, India. *International Journal of Pharma Bioscience and Technology, 4*(1), 515–523.
31. Tian, B., Hua, S., Liu, J. (2020). Cyclodextrin-based delivery systems for chemotherapeutic anticancer drugs: A review. *Carbohydrate Polymers, 232*, 115805. https://doi.org/10.1016/j.carbpol.2019.115805
32. Tu, X., Gao, F., Ma, X., Zou, J., Yu, Y., Li, M., Qu, F., Huang, X., Lu, L. (2020). Mxene/carbon nanohorn/β-cyclodextrin-Metal-organic frameworks as high-performance electrochemical sensing platform for sensitive detection of carbendazim pesticide. *Journal of Hazardous Materials*, 122776. https://doi.org/10.1016/j.jhazmat.2020.122776
33. Usta, J., Kreydiyyeh, S., Knio, K., Barnabe, P., Bou-Moughlabay, Y., Dagher, S. (2009). Linalool decreases HepG2 viability by inhibiting mitochondrial complexes I and II, increasing reactive oxygen species and decreasing ATP and GSH levels. *Chemico-Biological Interactions, 180*(1), 39–46. https://doi.org/10.1016/j.cbi.2009.02.012
34. Wang, Y., Jiang, Z.T., Li, R. (2009). Complexation and molecular microcapsules of *Litsea cubeba* essential oil with β-cyclodextrin and its derivatives. *European Food Research and Technology, 228*(6), 865–873. https://doi.org/10.1007/s00217-008-0999-3
35. Wang, Y., Li, R., Jiang, Z.T., Tan, J., Tang, S.H., Li, T.T., Liang, L.L., He, H.J., Liu, Y.M., Li, J.T., Zhang, X.C. (2018). Green and solvent-free simultaneous ultrasonic-microwave assisted extraction of essential oil from white and black peppers. *Industrial Crops and Products, 114*, 164–172. https://doi.org/10.1016/j.indcrop.2018.02.002
36. Wang, Y., Liu, T., Li, M.F., Yang, Y.S., Li, R., Tan, J., Tang, S.H., Jiang, Z.T. (2019). Composition, cytotoxicity and antioxidant activities of polyphenols in the leaves of star anise (*Illicium verum* Hook. f.). *ScienceAsia, 45*(6), 532–537. https://doi.org/10.2306/scienceasia1513-1874.2019.45.532
37. Wu, Y., Luo, Y., Zhou, B., Mei, L., Wang, Q., Zhang, B. (2019). Porous metal-organic framework (MOF) carrier for incorporation of volatile antimicrobial essential oil. *Food Control, 98*, 174–178. https://doi.org/10.1016/j.foodcont.2018.11.011
38. Xu, B., Chang, S.K. (2012). Comparative study on antiproliferation properties and cellular antioxidant activities of commonly consumed food legumes against nine human cancer cell lines. *Food Chemistry, 134*(3), 1287–1296. https://doi.org/10.1016/j.foodchem.2012.02.212
39. Yang, L.C., Li, R., Tan, J., Jiang, Z.T. (2013). Polyphenolics composition of the leaves of *Zanthoxylum bungeanum* Maxim. grown in Hebei, China, and their radical scavenging activities. *Journal of Agricultural and Food Chemistry, 61*(8), 1772–1778. https://doi.org/10.1021/jf3042825
40. Young, L., Sung, J., Stacey, G., Masters, J.R. (2010). Detection of mycoplasma in cell cultures. *Nature Protocol*, *5*(5), 929. https://doi.org/10.1038/nprot.2010.43
41. Yuan, C., Wang, Y., Liu, Y., Cui, B. (2019). Physicochemical characterization and antibacterial activity assessment of lavender essential oil encapsulated in hydroxypropyl-beta-cyclodextrin. *Industrial Crops and Products, 130*, 104–110. https://doi.org/10.1016/j.indcrop.2018.12.067
42. Zhao, Y., Chen, R., Wang, Y., Qing, C., Wang, W., Yang, Y. (2017). *In vitro* and *in vivo* efficacy studies of *Lavender angustifolia* essential oil and its active constituents on the proliferation of human prostate cancer. *Integrative Cancer Therapies, 16*(2), 215–226. https://doi.org/10.1177/1534735416645408

Submitted: 5 October 2020. Revised: 21 December 2020. Accepted: 31 December 2020. Published on-line: 25 January 2021.